

# A second-order generalization of TC and DC kernels

Mattia Zorzi<sup>a</sup>

<sup>a</sup>*Dipartimento di Ingegneria dell'Informazione, Università degli studi di Padova, via Gradenigo 6/B, 35131 Padova, Italy*

---

## Abstract

Kernel-based methods have been successfully introduced in system identification to estimate the impulse response of a linear system. Adopting the Bayesian viewpoint, the impulse response is modeled as a zero mean Gaussian process whose covariance function (kernel) is estimated from the data. The most popular kernels used in system identification are the tuned-correlated (TC), the diagonal-correlated (DC) and the stable spline (SS) kernel. TC and DC kernel admits a closed form factorization of the inverse and determinant which is inherently related to the fact that they solve a band extension problem, respectively, while maximizing the entropy. The SS kernel induces more smoothness than TC and DC on the estimated impulse response, however, the aforementioned properties do not hold in this case. In this paper we propose a second-order extension of the TC and DC kernel which induces more smoothness than TC and DC, respectively, on the impulse response. Moreover, these generalizations admit a closed form factorization of the inverse and determinant and represent the maximum entropy solution of a band extension problem, respectively. Interestingly, these new kernels belong to the family of the so called exponentially convex local stationary kernels: such a property allows to immediately analyze the frequency properties induced on the estimated impulse response by these kernels. Finally, numerical results show that the second-order TC kernel exhibits a performance similar to the one of the SS kernel. Thus, the former can represent an alternative to the latter in order to estimate the kernel hyperparameters in an efficient way.

*Key words:* Covariance extension; Gaussian process; kernel methods; maximum entropy; system identification.

---

## 1 Introduction

Linear system identification problems are traditionally addressed by using Prediction Error Methods (PEM), see Ljung (1999); Söderström & Stoica (1989). Here, the best model is chosen over a fixed parametric model class (e.g. ARMAX, OE, Box-Jenkins). This approach, however, has two issues: first, the parametrization of the predictor is nonlinear which implies that the minimization of the squared prediction error leads to a non-convex optimization problem; second, we have to face a model selection problem (i.e. order selection) which is usually performed by AIC and BIC criteria (Akaike, 1974; Schwarz, 1978).

Regularized kernel-based methods have been recently proposed in system identification in order to overcome the aforementioned limitations, see Pilonetto & De Nicolao (2010); Chen et al. (2012); Pilonetto et al. (2014). Here, we search the candidate model, described via the predictor impulse response, in an infinite dimensional nonparametric model class with the help of a penalty term. Adopting the Bayesian viewpoint, this

is a Gaussian process regression problem (Rasmussen & Williams, 2006): the impulse response is modeled as a Gaussian process with zero mean and with a suitable covariance function, also called kernel (Wahba, 1990). The latter encodes the a priori knowledge about the predictor impulse response. For instance, we would that the impulse is Bounded Input Bounded Output (BIBO) stable and with a certain degree of smoothness.

The most popular kernels are the tuned-correlated (TC), the diagonal-correlated (DC), and the stable-spline (SS). All these kernels encode the BIBO stability property. Regarding the smoothness, SS is the one inducing more smoothness on the impulse response. It is worth noting that many other extensions can be obtained, see for instance Chen & Ljung (2015a); Dinuzzo (2015); Zorzi & Chiuso (2018); Chen & Ljung (2015b); Zorzi (2020). All these kernels depend on few hyperparameters that are learnt from the data by minimizing the so called negative log-marginal likelihood. This task is computationally expensive especially in the case we want to estimate high dimensional models, e.g. the case of dynamic networks, see Zorzi & Chiuso (2017); Chiuso & Pilonetto (2012); Zorzi & Chiuso (2015).

To reduce the computational complexity different strate-

---

*Email address:* zorzi@dei.unipd.it (Mattia Zorzi).

gies have been proposed, see Carli et al. (2012); Chen et al. (2018); Chen & Andersen (2021); Chen & Ljung (2013a). In particular, if the kernel matrix admits a closed form expression for Cholesky factor of its inverse matrix as well as its determinant, then the evaluation of the marginal likelihood can be done efficiently (Chen & Ljung, 2013a).

It is worth noting that it is possible to derive these closed form expressions only for TC and DC, see Carli (2014); Carli et al. (2017). Moreover, TC and DC kernels have its inverse which is tridiagonal. The aforementioned properties are inherently related to the fact that the TC and DC kernels admit a precise maximum entropy interpretation: they solve a band extension problem while maximizing the entropy. It is worth noting that they also solve other maximum problems, see Chen et al. (2016); Chen (2018); Ardeshiri & Chen (2015), however, the latter do not lead to properties useful for implementation purposes. Unfortunately, the closed form expression for the Cholesky factor of the inverse and determinant as well as the corresponding band extension problem do not extend to the SS kernel.

The aim of this paper is introduce a second-order generalization of the TC and DC kernel exploiting the filter-based approach proposed in Marconato et al. (2017). These extensions induces more smoothness than TC and DC, respectively. Moreover, their inverse is pentadiagonal, they admit a closed form expression for the Cholesky of its inverse matrix and determinant. Moreover, these second-order extensions coincide with the maximum entropy solution of a band extension problem, respectively. It is worth noting that SS is the second-order extension of the TC kernel derived in the continuous time. In contrast, the extension that we propose here is derived in the discrete time. Numerical experiments showed that the new second-order TC kernel represents a good alternative to SS in terms of estimation performance. This idea can be also used to higher order extensions and also to generalize the high frequency kernel proposed in Pilonetto & De Nicolao (2011). Interestingly, all these new kernels are exponentially convex local stationary (ECLS) (Chen & Ljung, 2015a; Zorzi & Chiuso, 2018). Such a property allows to easily understand the frequency properties of their stationary parts.

The outline of the paper is as follows. In Section 2 we briefly review the kernel-based PEM method as well as the TC, DC and SS kernels. Section 3 introduces the second-order extension for the TC kernel, while Section 4 the one for the DC kernel. In Section 5 we show the maximum entropy properties of these new kernels. In Section 6 we extend this idea to higher order generalizations. In Section 7 we show that these kernels are ECLS and we analyze the stationary part of these kernels in the frequency domain. Some numerical experiments are provided in Section 8. Finally, we draw the conclusions in Section 9.

*Notation.*  $\mathcal{S}_T$ , with  $T \leq \infty$ , denotes the cone of positive definite symmetric matrices of dimension  $T \times T$ . Infinite dimensional matrices, i.e. matrices having an infinite number of columns and/or rows, are denoted using the calligraphic font, e.g.  $\mathcal{K}$ , while finite dimensional ones are denoted using the normal font, e.g.  $K$ . Given  $\mathcal{F} \in \mathbb{R}^{p \times \infty}$  and  $\mathcal{G} \in \mathbb{R}^{\infty \times m}$ , the product  $\mathcal{F}\mathcal{G}$  is understood as a  $p \times m$  matrix whose entries are limits of infinite sequences (Jorgesen et al., 2011). Given  $K \in \mathcal{S}_T$ ,  $[K]_{t,s}$  denotes the entry of  $K$  in position  $(t, s)$ , while  $[K]_{:,t}$  and  $[K]_{t,:}$  denotes the  $t$ -th column and row, respectively, of  $K$ . Given  $K \in \mathcal{S}_T$ ,  $\|v\|_{K^{-1}}$  denotes the weighted Euclidean norm of  $v$  with weight  $K^{-1}$ . Given  $v \in \mathbb{R}^T$ ,  $\text{Tpl}(v)$  denotes the lower triangular  $T \times T$  Toeplitz matrix whose first column is given by  $v$ , while  $\text{diag}(v)$  denotes the diagonal matrix whose main diagonal is  $v$ .

## 2 Kernel-based PEM method

Consider the model

$$y(t) = \sum_{k=1}^{\infty} g(k)u(t-k) + e(t), \quad t = 1 \dots N \quad (1)$$

where  $y(t)$ ,  $u(t)$ ,  $g(t)$  and  $e(t)$  denote the output, the input, the impulse response of the model and a zero-mean white Gaussian noise with variance  $\sigma^2$ , respectively. We can rewrite model (1) as

$$y = \mathcal{A}g + e$$

where  $y = [y(1) \dots y(N)]^T \in \mathbb{R}^N$ ,  $e$  is defined likewise,  $\mathcal{A}^{N \times \infty}$  is the regression matrix whose entries are defined by  $u(t)$  with  $t = 1 \dots N$ ,  $g = [g(1) g(2) \dots]^T \in \mathbb{R}^{\infty}$ . We want to estimate the impulse response  $g$  given the measurements  $\{y(t), u(t)\}_{t=1}^N$ . Such a problem is ill-posed because we have a finite number of measurements while  $g$  contains infinite parameters. The latter can be made well-posed assuming that  $g \sim \mathcal{N}(0, \lambda \mathcal{K}(\eta))$  where  $\mathcal{K}(\eta) \in \mathcal{S}_{\infty}$  is the kernel function; in this way, the minimum variance estimator of  $g$  is:

$$\hat{g} = \underset{g \in \mathbb{R}^{\infty}}{\text{argmin}} \|y - \mathcal{A}g\|^2 + \frac{\sigma^2}{\lambda} \|g\|_{\mathcal{K}(\eta)^{-1}}^2 \quad (2)$$

where  $\lambda > 0$  denotes the regularization parameter. It is worth noting that the above problem admits a closed form solution. Moreover,  $\mathcal{K}(\eta)$  encodes the a priori information that we have on the impulse response.

The aforementioned problem can be formulated as a finite dimensional problem. Indeed,  $g$  can be truncated, obtaining a finite impulse response of length  $T$ ; the corresponding kernel matrix  $K(\eta) \in \mathcal{S}_T$  is defined as  $[K(\eta)]_{t,s} = [\mathcal{K}(\eta)]_{t,s}$  for  $t, s = 1 \dots T$  and the regression matrix  $A \in \mathbb{R}^{N \times T}$  is given by the first  $T$  columns of  $\mathcal{A}$ .

Such a truncation, with  $T$  sufficiently large, does not introduce a bias, because  $g$  decays to zero. The so called hyperparameters  $\lambda$  and  $\eta$  are estimated by minimizing numerically the negative log-marginal likelihood

$$\ell(y; \lambda, \eta) := \log \det(\lambda AK(\eta)A^\top + \sigma^2 I) + y^\top (\lambda AK(\eta)A^\top + \sigma^2 I)^{-1} y. \quad (3)$$

In what follows, we will drop the dependence on  $\eta$  for kernels, unless it is required in order to avoid confusion.

### 2.1 Diagonal and correlated kernels: an overview

The simplest kernel is diagonal and encodes the a priori information that  $g$  should decay to zero exponentially:

$$\mathcal{K}_{DI} = \text{diag}(\beta, \beta^2, \dots, \beta^t, \dots) \quad (4)$$

where  $\eta = \beta$  and  $0 < \beta < 1$ . Indeed, the penalty term  $\|g\|_{\mathcal{K}_{DI}^{-1}}^2$  is the squared norm of the weighted impulse response

$$h = [h_1 \ h_2 \ \dots \ h_t \ \dots]^\top, \quad h_t = \beta^{-t/2} g_t$$

which amplifies in an exponential way the coefficients  $g_t$  as  $t$  increases. The tuned-correlated (TC, also called first-order stable spline) kernel embeds also the a priori information that  $g$  is smooth:

$$[\mathcal{K}_{TC}]_{t,s} = \beta^{\max(t,s)} \quad (5)$$

where  $\eta = \beta$  and  $0 < \beta < 1$ . The smoothness property can be justified as follows. It is well known that

$$\mathcal{K}_{TC} = (1 - \beta)(\mathcal{F}\mathcal{D}\mathcal{F}^\top)^{-1}$$

where

$$\mathcal{F} = \text{Tpl}(1, -1, 0, \dots) \\ \mathcal{D} = \text{diag}(\beta^{-1}, \beta^{-2}, \dots, \beta^{-t}, \dots);$$

then,  $\mathcal{F}^\top$  is the prefiltering operator performing the first order difference of  $h$  and thus the penalty term in (2) penalizes impulses responses for which the norm of the first order difference of the corresponding  $h$  is large

$$\|g\|_{\mathcal{K}_{TC}^{-1}}^2 = (1 - \beta)^{-1} \|\mathcal{F}^\top h\|^2 \\ = (1 - \beta)^{-1} \sum_{t=1}^{\infty} (h_t - h_{t+1})^2.$$

The diagonal-correlated (DC) kernel is defined as

$$[\mathcal{K}_{DC}]_{t,s} = \alpha^{|t-s|} \beta^{\max(t,s)} \quad (6)$$

where  $0 < \beta < 1$ ,  $-\beta^{-1/2} < \alpha < \beta^{-1/2}$  and  $\eta = [\alpha \ \beta]^\top$ . It is worth noting that we are taking a definition which is not standard, the standard one is  $[\mathcal{K}_{DC}]_{t,s} = \rho^{|t-s|} \beta^{\frac{t+s}{2}}$  and  $\rho = \alpha\beta^{1/2}$ , because the former highlights the following limits:

$$\lim_{\alpha \rightarrow 0} \mathcal{K}_{DC} = \mathcal{K}_{DI}, \quad \lim_{\alpha \rightarrow 1} \mathcal{K}_{DC} = \mathcal{K}_{TC}$$

that is the DC kernel connects the DI and TC kernel. Indeed, it is not difficult to see that

$$\mathcal{K}_{DC} = (1 - \alpha\beta)(\mathcal{F}_\alpha \mathcal{D} \mathcal{F}_\alpha^\top)^{-1}$$

with

$$\mathcal{F}_\alpha = \text{Tpl}(1, -\alpha, 0, \dots). \quad (7)$$

In plain words,  $\alpha$  tunes the behavior of the prefiltering operator:  $\mathcal{F}_\alpha^\top$  behaves as the identity operator for  $\alpha$  close to zero, while it behaves as the first order difference operator for  $\alpha$  close to one. As a consequence the DC kernel allows to tune the degree of smoothness of  $g$ .

All these kernels admit a closed form factorization, inverse and determinant which is an appealing feature for minimizing numerically (3). Moreover, their inverses are banded matrices:  $\mathcal{K}_{DI}^{-1}$  is diagonal,  $\mathcal{K}_{TC}^{-1}$  and  $\mathcal{K}_{DC}^{-1}$  are tridiagonal. The latter property reflects the fact that these kernels are, respectively, the maximum entropy solution of a band completion problem.

The stable spline (SS, also called second-order stable spline) kernel induces more smoothness than TC:

$$[\mathcal{K}_{SS}]_{t,s} = \frac{\gamma^{t+s} \gamma^{\max(t,s)}}{2} - \frac{\gamma^{3\max(t,s)}}{6} \quad (8)$$

where  $\eta = \gamma$  and  $0 < \gamma < 1$ . However, it does not admit a closed form factorization, inverse and determinant. Moreover, its inverse is not banded and thus such a kernel is not the maximum entropy solution of a matrix completion problem. Finally, it does not exist a kernel, with the aforementioned properties, which tunes the degree of smoothness and connects TC with SS.

### 3 Second-order TC kernel

In this section we derive a new kernel, hereafter called TC2, which induces more smoothness than TC and represents an alternative to SS. In order to induce more smoothness it is sufficient to take the penalty term as the norm of the second order difference of  $h$ :

$$\|g\|_{\mathcal{K}_{TC2}^{-1}}^2 = (1 - \beta)^{-3} \|(\mathcal{F}^\top)^2 h\|^2,$$

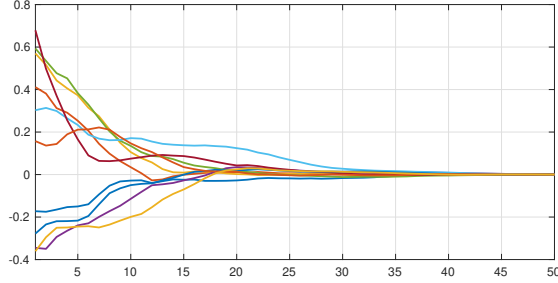


Fig. 1. Ten realizations of  $g \sim \mathcal{N}(0, \lambda \mathcal{K}_{TC2})$  with  $\beta = 0.8$  and  $\lambda = \|\mathcal{K}_{TC2}\|^{-1}$ .

thus

$$\mathcal{K}_{TC2} := (1 - \beta)^3 (\mathcal{F}^2 \mathcal{D} (\mathcal{F}^\top)^2)^{-1}$$

where  $\eta = \beta$  and  $0 < \beta < 1$ . Figure 1 shows ten realizations of  $g$  using the TC2 kernel with  $\beta = 0.8$ . We can notice that the degree of smoothness is similar to the one with  $\mathcal{K}_{SS}$ .

**Proposition 1** *The inverse of  $\mathcal{K}_{TC2}$  is a pentadiagonal matrix, that is  $[(\mathcal{K}_{TC2})^{-1}]_{t,s} = 0$  for any  $|t - s| > 3$ .*

**Proof.** The statement is a particular instance of Proposition 16, see Section 6. ■

Throughout the paper we will use the following result.

**Lemma 2 (Ford et al. (2014))** *Consider a real infinite lower triangular Toeplitz matrix, defined by the sequence  $\{a_k, k \geq 0\}$  as follows*

$$\mathcal{X} = \text{Tpl}(a_0, a_1, a_2, \dots).$$

*If  $a_0 \neq 0$ ,  $\mathcal{X}$  is invertible and the inverse matrix  $\mathcal{Y} = \mathcal{X}^{-1}$  is also a lower triangular Toeplitz matrix with elements  $\{b_k, k \geq 0\}$  given by the following formula*

$$b_0 = \frac{1}{a_0}, \quad b_k = -\frac{1}{a_0} \sum_{j=0}^{k-1} a_{k-j} b_j \text{ for } k \geq 1.$$

**Proposition 3**  $\mathcal{K}_{TC2}$  admits the following closed form expression:

$$[\mathcal{K}_{TC2}]_{t,s} = 2\beta^{\max(t,s)+1} + (1 - \beta)(1 + |t - s|)\beta^{\max(t,s)}. \quad (9)$$

**Proof.** First,  $\mathcal{F}$  is a lower triangular Toeplitz matrix which is invertible because the main diagonal is composed by strictly positive elements. Therefore, by Lemma 2 we have

$$\mathcal{F}^{-2} = \text{Tpl}(1, 2, \dots, t, \dots).$$

Moreover,

$$[\mathcal{F}^{-2}]_{t,:} = [0 \ \dots \ 0 \ \underbrace{1}_{t\text{-th element}} \ 2 \ 3 \ \dots].$$

Therefore,

$$\begin{aligned} [\mathcal{K}_{TC2}]_{t,s} &= (1 - \beta)^3 [(\mathcal{F}^{-2})^\top \mathcal{D}^{-1} \mathcal{F}^{-2}]_{t,s} \\ &= (1 - \beta)^3 [\mathcal{F}^{-2}]_{t,:} \mathcal{D}^{-1} [(\mathcal{F}^\top)^{-2}]_{:,s} \\ &= (1 - \beta)^3 [\mathcal{F}^{-2}]_{t,:} \mathcal{D}^{-1} [\mathcal{F}^{-2}]_{s,:}^\top \\ &= \sum_{k=\max(t,s)}^{\infty} \beta^k (k - t + 1)(k - s + 1). \end{aligned}$$

Finally, it is not difficult to see that the above series converges to (9) by exploiting the identity

$$\sum_{k=0}^{\infty} \beta^k = \frac{1}{1 - \beta}. \quad (10)$$

■

It is worth noting that the SS kernel is also a second-order generalization of the TC kernel. Indeed, TC and SS are obtained by applying a “stable” coordinate change to the first and second order, respectively, spline kernel (Pillonetto & De Nicolao, 2010). That extension has been derived in the continuous time domain, while the one proposed here has been derived in the discrete time domain.

## 4 Second-order DC kernel

The aim of this section is to introduce a new kernel, hereafter called DC2, which connects the TC and TC2 kernels. The unique difference between TC and TC2 is the prefiltering operator acting on  $h$ . Thus, the DC2 kernel should perform a transition from  $\mathcal{F}$  to  $\mathcal{F}^2$ . One possible way is to take

$$\mathcal{F}_{2,\alpha} := (1 - \alpha)\mathcal{F} + \alpha\mathcal{F}^2 \quad (11)$$

with  $0 \leq \alpha \leq 1$  and thus we obtain

$$\mathcal{K}_{DC2} := \kappa (\mathcal{F}_{2,\alpha} \mathcal{D} \mathcal{F}_{2,\alpha}^\top)^{-1} \quad (12)$$

with  $\kappa = (1 - \beta)(1 - \alpha\beta)(1 - \alpha^2\beta)$ . In this case we have  $\eta = [\alpha \ \beta]^\top$  with  $0 < \beta < 1$ . From the above definition it follows that

$$\lim_{\alpha \rightarrow 0} \mathcal{K}_{DC2} = \mathcal{K}_{TC}, \quad \lim_{\alpha \rightarrow 1} \mathcal{K}_{DC2} = \mathcal{K}_{TC2}.$$

Figure 2 shows a realization of the impulse response as a function of  $\alpha$  using (12); as expected, the degree of smoothness increases as  $\alpha$  increases.

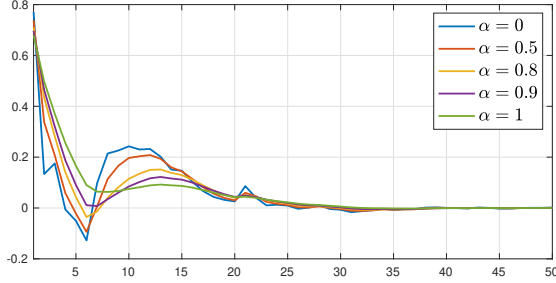


Fig. 2. One realization of  $g \sim \mathcal{N}(0, \lambda \mathcal{K}_{DC2})$  for different values of  $\alpha$ . Here,  $\lambda = \|\mathcal{K}_{DC2}\|^{-1}$ .

**Remark 4** *It is worth noting that one could consider other transitions, e.g.*

$$\begin{aligned} \mathcal{F}_{2,\alpha} &= \text{Tpl}(1, -1 - \alpha^2, \alpha, 0, \dots) \\ \mathcal{F}_{2,\alpha} &= ((1 - \alpha)\mathcal{F}^{-1} + \alpha\mathcal{F}^{-2})^{-1}. \end{aligned}$$

However, as we will see, (11) is the unique definition which guarantees that  $K_{DC2}$  admits a closed form expression and is the maximum entropy solution of a matrix completion problem.

**Proposition 5** *The inverse of  $\mathcal{K}_{DC2}$  is a pentadiagonal matrix, that is  $[(\mathcal{K}_{DC2})^{-1}]_{t,s} = 0$  for any  $|t - s| > 3$ .*

**Proof.** The proof is similar to the one of Proposition 1. ■

**Proposition 6** *For  $0 \leq \alpha < 1$ ,  $\mathcal{K}_{DC2}$  admits the following closed form expression:*

$$[\mathcal{K}_{DC2}]_{t,s} = \frac{\beta^{\max(t,s)}(1 - (1 - \beta)\alpha^{|t-s|+1}) - \alpha^2\beta^{\max(t,s)+1}}{1 - \alpha}. \quad (13)$$

**Proof.** First, we notice that

$$\mathcal{F}_{2,\alpha} = ((1 - \alpha)\mathcal{I} + \alpha\mathcal{F})\mathcal{F} = \mathcal{F}_\alpha\mathcal{F}$$

where  $\mathcal{F}_\alpha$  has been defined in (7);  $\mathcal{I}$  is the identity matrix of infinite dimension. The main diagonal of  $\mathcal{F}$  and  $\mathcal{F}_\alpha$  is composed by strictly positive elements and thus their inverse exist. By Lemma 2, we have

$$\begin{aligned} \mathcal{F}^{-1} &= \text{Tpl}(1, 1, \dots) \\ \mathcal{F}_\alpha^{-1} &= \text{Tpl}(1, \alpha, \alpha^2, \dots). \end{aligned}$$

Therefore,

$$\mathcal{F}_{2,\alpha}^{-1} = \frac{1}{1 - \alpha} \text{Tpl}(1 - \alpha, 1 - \alpha^2, 1 - \alpha^3, \dots).$$

Finally,

$$\begin{aligned} [\mathcal{K}_{DC2}]_{t,s} &= \kappa[\mathcal{F}_{2,\alpha}^{-1}]^\top \mathcal{D}[\mathcal{F}_{2,\alpha}^{-1}]_{:,s} \\ &= \kappa \sum_{k=\max(t,s)}^{\infty} \beta^k \frac{1 - \alpha^{k-t+1}}{1 - \alpha} \frac{1 - \alpha^{k-s+1}}{1 - \alpha} \end{aligned}$$

where the above series converges to right hand side of (13). The latter fact can be easily proved by using Identity (10). ■

## 5 Maximum entropy properties

The aim of this section is to prove that  $K_{TC2} \in \mathcal{S}_T$  and  $K_{DC2} \in \mathcal{S}_T$ , with  $T \geq 4$ , are the maximum entropy solution of a matrix completion problem, more precisely a band extension problem. Recall that the finite dimensional kernels  $K_{TC2}$  and  $K_{DC2}$  are submatrices of  $\mathcal{K}_{TC2}$  and  $\mathcal{K}_{DC2}$ , respectively:

$$\begin{aligned} [K_{TC2}]_{t,s} &= [\mathcal{K}_{TC2}]_{t,s} \\ [K_{DC2}]_{t,s} &= [\mathcal{K}_{DC2}]_{t,s}, \quad t, s = 1 \dots T. \end{aligned}$$

Before to prove the aforementioned property, we need to introduce the background.

**Problem 7 (Band extension problem)** *Given  $m$  and  $c_{t,s}$ , with  $|t - s| \leq m$ , find the covariance matrix  $\Sigma \in \mathcal{S}_T$  of a zero mean Gaussian random vector such that*

$$[\Sigma]_{t,s} = c_{t,s}, \quad |t - s| \leq m.$$

The maximum entropy solution (or extension) of the above problem is defined as

$$\begin{aligned} \min_{\Sigma \in \mathcal{S}_T} \log \det \Sigma \\ \text{subject to } [\Sigma]_{t,s} = c_{t,s}, \quad |t - s| \leq m. \end{aligned} \quad (14)$$

As pointed out by Dempster in Dempster (1972), “the principle of seeking maximum entropy is a principle of seeking maximum simplicity of explanation”.

**Proposition 8 (Dym & Gohberg (1981))** *Problem (14) admits solution if and only if*

$$\begin{bmatrix} c_{t,t} & \dots & c_{t,m+t} \\ \vdots & & \vdots \\ c_{t+m,t} & \dots & c_{t+m,t+m} \end{bmatrix} \in \mathcal{S}_{m+1}, \quad t = 1 \dots T - m.$$

*Under such assumption, the solution is unique with the additional property that its inverse is banded of bandwidth  $m$ , i.e. its elements in position  $(t, s)$  are zero for  $|t - s| > m$ .*

The maximum entropy extension admits a closed form solution that can be computed recursively as follows. Let  $\Sigma_T^{(T-2)}$  be the partially specified  $T \times T$  symmetric matrix

$$\Sigma_T^{(T-2)} = \begin{bmatrix} c_{1,1} & c_{1,2} & \dots & c_{1,T-1} & x \\ c_{1,2} & c_{2,2} & \dots & c_{2,T-1} & c_{2,T} \\ \vdots & \vdots & & \vdots & \vdots \\ c_{1,T-1} & c_{2,T-1} & \dots & c_{T-1,T-1} & c_{T-1,T} \\ x & c_{2,T} & \dots & c_{T-1,T} & c_{T,T} \end{bmatrix} \quad (15)$$

where  $x$  is not fixed. Let  $L \in \mathcal{S}_{T-1}$  be the submatrix of  $\Sigma_T^{(T-2)}$  such that

$$[L]_{t,s} = c_{t,s}, \quad t, s = 1 \dots T-1.$$

In what follows, the solution of (14) with  $m = T-2$  will be called one-step extension.

**Proposition 9 (Gohberg et al. (1993))** *The following facts hold:*

i) *The one-step extension is given by (15) with*

$$x = -\frac{1}{y_1} \sum_{j=2}^{T-1} c_{T,j} y_j \quad (16)$$

and

$$[y_1 \ y_2 \ \dots \ y_{T-1}]^\top = L^{-1}[1 \ 0 \ \dots \ 0]^\top;$$

ii) *The maximum entropy extension  $\Sigma_{ME}$  solution to (14) is such that  $\Sigma_{ME}^{-1}$  is a band matrix of bandwidth  $m$  and for all  $m+1 < t \leq T$  and  $1 \leq s \leq t-m-1$  the submatrix  $P^\circ \in \mathcal{S}_{t-s+1}$ , with  $[P^\circ]_{i,j} = [\Sigma_{ME}]_{s-1+i, s-1+j}$ , is the one-step extension of the problem*

$$\begin{aligned} & \min_{P \in \mathcal{S}_{t-s+1}} \log \det P \\ & \text{subject to } [P]_{i,j} = c_{s-1+i, s-1+j}, \quad |i-j| \leq t-s-1. \end{aligned}$$

### 5.1 TC2 kernel

In order to illustrate the main result we need the following proposition.

**Proposition 10** *The inverse of  $K_{TC2} \in \mathcal{S}_T$  admits the following decomposition*

$$K_{TC2}^{-1} = (1-\beta)^{-3} F_T^2 D_T (F_T^2)^\top$$

where

$$\begin{aligned} F_T &= \text{Tpl}(1, -1, 0, \dots, 0) \in \mathbb{R}^{T \times T} \\ D_T &= \begin{bmatrix} D_{1,T} & 0 \\ 0 & B_T \end{bmatrix} \\ D_{1,T} &= \text{diag}(\beta^{-1}, \beta^{-2}, \dots, \beta^{T-2}) \\ B_T &= (1-\beta)\beta^{-T} \begin{bmatrix} \beta + \beta^2 & 2\beta^2 \\ 2\beta^2 & 1 - 3\beta + 4\beta^2 \end{bmatrix}. \end{aligned}$$

Thus,  $K_{TC2}^{-1}$  is a pentadiagonal matrix.

**Proof.** Consider

$$X := (1-\beta)^3 (F_T^2 \tilde{D}_T (F_T^2)^\top)^{-1}$$

where

$$\tilde{D}_T = \text{diag}(\beta^{-1}, \beta^{-2}, \dots, \beta^{-T}). \quad (17)$$

It is not difficult to see that

$$F_T^{-2} = \text{Tpl}(1, 2, \dots, T).$$

Thus, by arguments similar to ones used in proof of Proposition 3, we have

$$[X]_{t,s} = (1-\beta)^3 \sum_{k=\max(t,s)}^T \beta^k (k-t+1)(k-s+1).$$

Without loss of generality, we assume that  $t \geq s$ ; hence,

$$\begin{aligned} [X]_{t,s} &= (1-\beta)^3 \sum_{k=t}^T \beta^k (k-t+1)(k-s+1) \\ &= (2\beta + (1-\beta)(1+t-s))\beta^t + \eta(t,s) \end{aligned}$$

where

$$\begin{aligned} \eta(t,s) &= (1-\beta)(\beta^{T+2}(T-t+1)(T-s+3) \\ &\quad - \beta^{T+1}(T-t+2)(T-s+2)) \\ &\quad + 2\beta^{T+2}((T-t+1)\beta - (T-t+2)) \end{aligned}$$

where we have exploited the fact that

$$\sum_{k=0}^T \beta^k = \frac{1-\beta^{T+1}}{1-\beta}.$$

Notice that

$$[K_{TC2}]_{t,s} = [X]_{t,s} - \eta(t,s)$$

and we can rewrite  $\eta$  in the shorthand way

$$\eta(t, s) = \gamma_1 t + \gamma_1 s + \gamma_2 ts + \gamma_3 \quad (18)$$

where  $\gamma_k$ 's are constants not depending on  $t$  and  $s$ . On the other hand, if we take

$$\begin{aligned} Y &:= (1 - \beta)^3 (F_T^2 \Delta^{-1} (F_T^2)^\top)^{-1} \\ &= (1 - \beta)^3 (F_T^{-2})^\top \Delta F_T^{-2}, \end{aligned}$$

with

$$\Delta = \begin{bmatrix} 0 & \dots & 0 & \dots & 0 \\ \vdots & \ddots & \vdots & & \vdots \\ \vdots & & 0 & z & y \\ 0 & \dots & 0 & y & x \end{bmatrix}, \quad (19)$$

then it is not difficult to see that

$$\begin{aligned} [Y]_{t,s} &= (1 - \beta)^3 [-T(x + 2y + z) + x + y](t + s) \\ &\quad + (x + 2y + z)ts + 2T(x + y) + x]. \end{aligned}$$

By taking into account (18), we can impose that  $x, y, z$  obey the conditions

$$\begin{aligned} \gamma_1 &= -(1 - \beta)^3 (T(x + 2y + z) + x + y) \\ \gamma_2 &= (1 - \beta)^3 (x + 2y + z) \\ \gamma_3 &= (1 - \beta)^3 [2T(x + y) + x]. \end{aligned}$$

In this way,  $\eta(t, s) = [Y]_{t,s}$ . With this choice, we have

$$\begin{aligned} K_{TC2} &= X - Y = (1 - \beta)^3 (F_T^{-2})^\top (\tilde{D}_T^{-1} - \Delta) (F_T^{-2}) \\ &= (1 - \beta)^3 (F_T^2 (\tilde{D}_T^{-1} - \Delta)^{-1} (F_T^2)^\top)^{-1} \end{aligned}$$

where it is not difficult to see that  $(\tilde{D}_T^{-1} - \Delta)^{-1}$  coincides with  $D_T$ . Finally, the fact that  $K_{TC2}^{-1}$  is pentadiagonal follows from Proposition 17, see Section 6.  $\blacksquare$

**Theorem 11** Consider Problem 7 with  $m = 2$  and

$$c_{t,s} = 2\beta^{\max(t,s)+1} + (1 - \beta)(1 + |t - s|)\beta^{\max(t,s)},$$

with  $|t - s| \leq 2$ . Then, the maximum entropy extension solution to (14) is  $K_{TC2}$ .

**Proof.** We prove the claim by using Proposition 9. First, by Proposition 10 we know that  $K_{TC2}^{-1}$  is banded

of bandwidth  $m = 2$ . Let

$$P(s, t) = \begin{bmatrix} c_{s,s} & c_{s,s+1} & \dots & c_{s,t-1} & c_{s,t} \\ c_{s,s+1} & c_{s+1,s+1} & \dots & c_{s+1,t-1} & c_{s+1,t} \\ \vdots & \vdots & & \vdots & \vdots \\ c_{s,t-1} & c_{s+1,t-1} & \dots & c_{t-1,t-1} & c_{t-1,t} \\ c_{s,t} & c_{s+1,t} & \dots & c_{t-1,t} & c_{t,t} \end{bmatrix}, \quad (20)$$

with  $m + 1 < t \leq T$  and  $1 \leq s \leq t - m - 1$ , be the submatrix of  $K_{TC2}$ . Then, given the particular definition of  $c_{t,s}$ 's, it is not difficult to see that

$$\begin{aligned} P(s, t) &= \beta^{s-1} P(1, t - s + 1) \\ &= \beta^{s-1} (1 - \beta)^3 (F_{t-s+1}^2 D_{t-s+1} (F_{t-s+1}^2)^\top)^{-1} \end{aligned}$$

where the last equality follows by Proposition 10 with  $T = t - s + 1$ . By Proposition 9 we know that  $P$  is the one step-extension of the corresponding band extension problem if  $c_{s,t}$  is equal to  $x$  and the latter is given as follows. We define

$$\begin{aligned} &[y_1 \ y_2 \ \dots \ y_{t-s}]^\top \\ &= \beta^{1-s} (1 - \beta)^{-3} F_{t-s}^2 D_{t-s} (F_{t-s}^2)^\top [1 \ 0 \ \dots \ 0]^\top \\ &= \beta^{1-s} (1 - \beta)^{-3} [\beta^{-1} \ -2\beta^{-1} \ \beta^{-1} \ 0 \ \dots \ 0]^\top; \end{aligned}$$

therefore

$$\begin{aligned} x &= -\beta(-2\beta^{-1}c_{s+1,t} + \beta^{-1}c_{s+2,t}) = 2c_{s+1,t} - c_{s+2,t} \\ &= 2\beta^{t+1} + (1 - \beta)(1 + t - s)\beta^t = [K_{TC2}]_{t,s} \end{aligned}$$

which concludes the proof.  $\blacksquare$

## 5.2 DC2 kernel

In order to illustrate the main result we need the following proposition.

**Proposition 12** The inverse of  $K_{DC2} \in \mathcal{S}_T$  admits the following decomposition

$$K_{DC2}^{-1} = \kappa^{-1} F_{2,\alpha,T} D_T F_{2,\alpha,T}^\top$$

where

$$F_{2,\alpha,T} = (1 - \alpha)F_T + \alpha F_T^2$$

$$D_T = \begin{bmatrix} D_{1,T} & 0 \\ 0 & B_T \end{bmatrix}$$

$$D_{1,T} = \text{diag}(\beta^{-1}, \beta^{-2}, \dots, \beta^{T-2})$$

$$B_T = (1 - \alpha\beta)\beta^{-T}$$

$$\times \begin{bmatrix} \beta(1 + \alpha\beta) & \alpha\beta^2(1 + \alpha) \\ \alpha\beta^2(1 + \alpha) & (1 - \beta - \alpha^2\beta)(1 - \alpha\beta) + 2\alpha^2\beta^2 \end{bmatrix}.$$

Thus,  $K_{DC2}^{-1}$  is a pentadiagonal matrix.

**Proof.** Consider

$$X := \kappa(F_{2,\alpha,T} \tilde{D}_T F_{2,\alpha,T}^\top)^{-1}$$

where  $\tilde{D}_T$  has been defined in (17). Notice that  $F_{2,\alpha,T} = F_{\alpha,T} F_T$  where

$$F_{\alpha,T} = \text{Tpl}(1, -\alpha, 0, \dots, 0) \in \mathbb{R}^{T \times T}$$

and

$$\begin{aligned} F_{\alpha,T}^{-1} &= \text{Tpl}(1, \alpha^2, \dots, \alpha^T) \\ F_{2,\alpha,T}^{-1} &= F_T^{-1} F_{\alpha,T}^{-1} \\ &= \frac{1}{1-\alpha} \text{Tpl}(1-\alpha, 1-\alpha^2, \dots, 1-\alpha^T). \end{aligned}$$

Without loss of generality, we assume that  $t \geq s$ , then it is not difficult to see that

$$\begin{aligned} [X]_{t,s} &= [(F_T^{-1})^\top (F_{\alpha,T}^{-1})^\top \tilde{D}_T^{-1} F_{\alpha,T}^{-1} F_T^{-1}]_{t,s} \\ &= \frac{1}{(1-\alpha)^2} \sum_{k=t}^T \beta^k (1-\alpha^{k-t+1})(1-\alpha^{k-s+1}) \\ &= [K_{DC2}]_{t,s} + \eta(t,s) \end{aligned}$$

where

$$\eta(t,s) = \gamma_1 \alpha^{-t} + \gamma_2 \alpha^{-s} + \gamma_3 \alpha^{-(t+s)} + \gamma_4 \quad (21)$$

and  $\gamma_k$ 's are constants not depending on  $t$  and  $s$ . On the other hand, if we take

$$\begin{aligned} Y &:= \kappa(F_{2,\alpha,T} \Delta^{-1} F_{2,\alpha,T}^\top)^{-1} \\ &= \kappa(F_{2,\alpha,T}^{-1})^\top \Delta F_{2,\alpha,T}^{-1} \end{aligned}$$

where  $\Delta$  is defined as in (19), then it is not difficult to see that

$$\begin{aligned} [Y]_{t,s} &= \kappa[-\alpha^T(z+y+\alpha x+\alpha y)(\alpha^{-t}+\alpha^{-s}) \\ &\quad + \alpha^{2T}(z+2\alpha y+\alpha^2 x)\alpha^{-(t+s)} + (z+2y+x)]. \end{aligned}$$

By taking into account (21), we can impose that  $x, y, z$  obey the conditions

$$\begin{aligned} \gamma_1 &= -\kappa \alpha^T (z+y+\alpha x+\alpha y) \\ \gamma_2 &= \kappa \alpha^{2T} (z+2\alpha y+\alpha^2 x) \\ \gamma_3 &= \kappa (z+2y+x). \end{aligned}$$

In this way,  $\eta(t,s) = [Y]_{t,s}$ . With this choice, we have

$$\begin{aligned} K_{DC2} &= X - Y = \kappa(F_{2,\alpha,T}^{-1})^\top (\tilde{D}_T^{-1} - \Delta) F_{2,\alpha,T}^{-1} \\ &= \kappa(F_{2,\alpha,T} (\tilde{D}_T^{-1} - \Delta)^{-1} F_{2,\alpha,T}^\top)^{-1} \end{aligned}$$

where it is not difficult to see that  $(\tilde{D}_T^{-1} - \Delta)^{-1}$  coincides with  $D_T$ . Finally, the fact that  $K_{DC2}^{-1}$  is pentadiagonal follows by Proposition 19 in Section 6. ■

**Theorem 13** Consider Problem 7 with  $m = 2$  and

$$c_{t,s} = \frac{\beta^{\max(t,s)}(1 - (1-\beta)\alpha^{|t-s|+1}) - \alpha^2 \beta^{\max(t,s)+1}}{1-\alpha},$$

with  $|t-s| \leq 2$ . Then, the maximum entropy extension solution to (14) is  $K_{DC2}$ .

**Proof.** We prove the claim by using Proposition 9. First, by Proposition 12 we know that  $K_{DC2}^{-1}$  is banded of bandwidth  $m = 2$ . Let  $P(t,s)$  be the submatrix of  $K_{DC2}$  defined as in (20) with  $m+1 < t \leq T$  and  $1 \leq s \leq t-m-1$ . Then, given the particular definition of  $c_{t,s}$ 's, it is not difficult to see that

$$\begin{aligned} P(s,t) &= \beta^{s-1} P(1, t-s+1) \\ &= \beta^{s-1} \kappa(F_{2,\alpha,t-s+1} D_{t-s+1} F_{2,\alpha,t-s+1}^\top)^{-1} \end{aligned}$$

where the last equality follows by Proposition 12 with  $T = t-s+1$ . By Proposition 9 we know that  $P$  is the one step-extension of the corresponding band extension problem if  $c_{s,t}$  is equal to  $x$  and the latter is given as follows. We define

$$\begin{aligned} [y_1 \ y_2 \ \dots \ y_{t-s}]^\top &= \beta^{1-s} \kappa^{-1} F_{2,\alpha,t-s} D_{t-s} F_{2,\alpha,t-s}^\top [1 \ 0 \ \dots \ 0]^\top \\ &= \beta^{1-s} \kappa^{-1} [\beta^{-1} \ - (1+\alpha)\beta^{-1} \ \alpha\beta^{-1} \ 0 \ \dots \ 0]^\top; \end{aligned}$$

therefore

$$\begin{aligned} x &= -\beta(-(1+\alpha)\beta^{-1}c_{s+1,T} + \alpha\beta^{-1}c_{s+2,T}) \\ &= (1+\alpha)c_{s+1,t} - \alpha c_{s+2,t} \\ &= \frac{\beta^t(1 - (1-\beta)\alpha^{t-s+1}) - \alpha^2 \beta^t}{1-\alpha} = [K_{DC2}]_{t,s} \end{aligned}$$

which concludes the proof. ■

### 5.3 Efficient and robust marginal likelihood evaluation

Kernel matrices can be very ill-posed and thus we need to take some care for minimizing the negative log-marginal likelihood in (3). The latter can be evaluated as follows, see Chen & Ljung (2013b):

$$\frac{r^2}{\sigma^2} + (N-T) \log \sigma^2 + \log \det(\lambda K) + 2 \log \det R_1 \quad (22)$$



where  $L$  is the Cholesky factor of  $K^{-1} = LL^T$  and  $R_1$  is given by the QR factorization

$$\begin{bmatrix} A & y \\ \sigma\sqrt{\lambda^{-1}}L^\top & 0 \end{bmatrix} = QR = Q \begin{bmatrix} R_1 & R_2 \\ 0 & r \end{bmatrix}$$

where  $Q^\top Q = I_{T+1}$ ,  $R_1 \in \mathbb{R}^{T \times T}$ ,  $R_2 \in \mathbb{R}^T$  and  $r \in \mathbb{R}$ . As explained in Carli et al. (2017), in the case that we have  $L$  and  $\log \det(\lambda K)$  in closed form, e.g. for TC and DC kernels, then (22) is an efficient and robust way to evaluate  $\ell$ . It is also worth noting that it is possible to perform a reduced QR factorization by computing only once the QR factorization of  $[A \ y]$ , see Chen & Ljung (2013b) for more details.

In what follows we show that also TC2 and DC2 have a closed form expression for  $L$  and  $\log \det(\lambda K)$ . Indeed, by Proposition 10 and 12 we have following corollaries.

**Corollary 14** *Let  $L$  denote the Cholesky factor of  $K_{TC2}^{-1}$ , then*

$$[L]_{t,s} = \begin{cases} \frac{1}{\sqrt{(1-\beta)^3\beta^t}}, & 1 \leq t = s \leq T-2 \\ \frac{-2}{\sqrt{(1-\beta)^3\beta^{t-1}}}, & 2 \leq t = s+1 \leq T-1 \\ \frac{1}{\sqrt{(1-\beta)^3\beta^{t-2}}}, & 3 \leq t = s+2 \leq T \\ \frac{\sqrt{\beta^{-T+1}(1+\beta)}}{\sqrt{(1-\beta)^3\beta^{t-1}}}, & t = s = T-1 \\ \frac{-2\sqrt{\beta^{-T+1}}}{(1-\beta)\sqrt{1+\beta}}, & t = s+1 = T \\ \sqrt{\frac{\beta^{-T}}{1+\beta}}, & t = s = T \\ 0, & \text{otherwise.} \end{cases}$$

Moreover,

$$\det K_{TC2} = \beta^{\frac{T(T+1)}{2}} (1-\beta)^{3T-4}.$$

**Corollary 15** *Let  $L$  denote the Cholesky factor of  $K_{DC2}^{-1}$ , then*

$$[L]_{t,s} = \begin{cases} \frac{1}{\sqrt{\kappa\beta^t}}, & 1 \leq t = s \leq T-2 \\ \frac{-(1+\alpha)}{\sqrt{\kappa\beta^{t-1}}}, & 2 \leq t = s+1 \leq T-1 \\ \frac{\alpha}{\sqrt{\kappa\beta^{t-2}}}, & 3 \leq t = s+2 \leq T \\ \sqrt{\frac{(1+\alpha\beta)\beta^{-T+1}}{(1-\beta)(1-\alpha^2\beta)}}, & t = s = T-1 \\ \frac{-(1+\alpha)\sqrt{\beta^{-T+1}}}{\sqrt{(1+\alpha\beta)(1-\beta)(1-\alpha^2\beta)}}, & t = s+1 = T \\ \sqrt{\frac{\beta^{-T}}{1+\alpha\beta}}, & t = s = T \\ 0, & \text{otherwise.} \end{cases}$$

Moreover,

$$\det K_{DC2} = \beta^{\frac{T(T+1)}{2}} (1-\alpha\beta)^{T-2} (1-\beta)^{T-1} (1-\alpha^2\beta)^{T-1}.$$

In view of the above properties, we have

$$\begin{aligned} \log \det(\lambda K_{TC2}) &= T \log \lambda + \frac{T(T+1)}{2} \log \beta \\ &\quad + (3T-4) \log(1-\beta) \\ \log \det(\lambda K_{DC2}) &= T \log \lambda + \frac{T(T+1)}{2} \log \beta \\ &\quad + (T-2) \log(1-\alpha\beta) + (T-1) \log(1-\beta) \\ &\quad + (T-1) \log(1-\alpha^2\beta). \end{aligned}$$

The closed form expression for the Cholesky factor of the inverse kernel matrix as well as its pentadiagonal structure can be also exploited to derive the closed form expression of the inverse kernel matrix. Moreover, these results can be exploited to compute efficiently the gradient and the Hessian of the kernel matrix with respect to the hyperparameters, see Remark V.2 in Carli et al. (2017). The latter, indeed, can be used to speed up the search of the minimum of (3) through gradient/Hessian based solvers.

Finally, the fact that the inverse kernel matrix is pentadiagonal can be also used to compute efficiently (2) through the alternating direction method of multipliers (ADMM) proposed in Fujimoto (2021). Indeed, although that paper considers the case of tridiagonal inverse kernel matrices (e.g. TC and DC kernels) that idea holds also for banded inverse kernel matrices and the computational flops do not change.

## 6 Higher-order extensions

Drawing inspiration from Section 3 we can define the TC kernel of order  $\delta \in \mathbb{N}$  as

$$\mathcal{K}_{TC\delta} = \kappa_\delta (\mathcal{F}^\delta \mathcal{D} (\mathcal{F}^\delta)^\top)^{-1} \quad (23)$$

where  $\kappa_\delta$  is a suitable normalization constant. Here,  $\eta = \beta$  with  $0 < \beta < 1$ . Figure 3 shows ten realizations of  $g$  using the  $\mathcal{TC}\delta$  kernel with  $\beta = 0.8$  and for different values of  $\delta$ . As expected, the larger  $\delta$  is the more smoothness is induced on  $g$ .

**Proposition 16** *The inverse of  $\mathcal{K}_{TC\delta}$  is a banded matrix of bandwidth  $\delta$ , that is  $[\mathcal{K}_{TC\delta}^{-1}]_{t,s} = 0$  for any  $|t-s| > \delta$ .*

**Proof.** We prove the claim by induction. First, for  $\delta = 1$  we have that  $\mathcal{TC}\delta$  is the standard TC and its inverse is

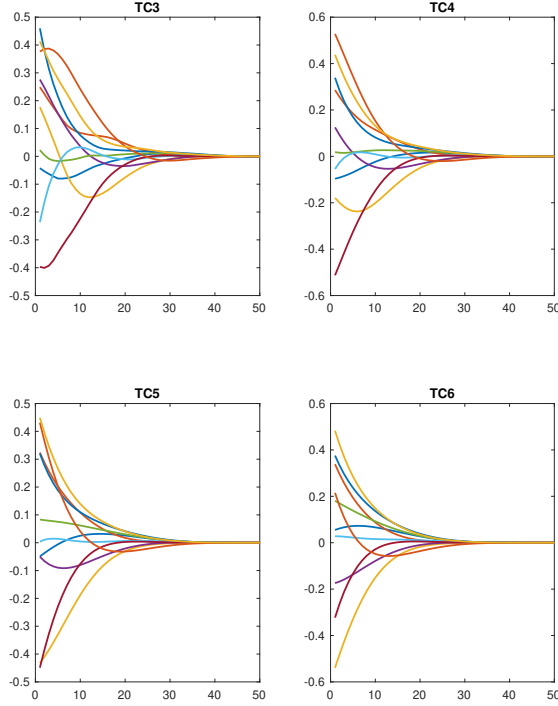


Fig. 3. Ten realizations of  $g \sim \mathcal{N}(0, \lambda \mathcal{K}_{TC\delta})$  with  $\beta = 0.8$ ,  $\delta = 3, 4, 5, 6$  and  $\lambda = \|\mathcal{K}_{TC\delta}\|^{-1}$ .

tridiagonal, i.e. the claim holds. Assume that  $\mathcal{K}_{TC\delta-1}^{-1}$  is a banded matrix of bandwidth  $\delta - 1$ . Then,

$$\mathcal{K}_{TC\delta}^{-1} = \frac{\kappa_{\delta-1}}{\kappa_{\delta}} \mathcal{F} \mathcal{K}_{TC\delta-1}^{-1} \mathcal{F}^{\top}.$$

Notice that  $\mathcal{F} = \mathcal{I} - \mathcal{S}$  where  $\mathcal{S}$  is the lower shift matrix and  $\mathcal{I}$  the identity matrix, both infinite dimensional. Hence,

$$\begin{aligned} \mathcal{K}_{TC\delta}^{-1} &= \kappa_{\delta-1} \kappa_{\delta}^{-1} [\mathcal{K}_{TC\delta-1}^{-1} \\ &+ \mathcal{S} \mathcal{K}_{TC\delta-1}^{-1} \mathcal{S}^{\top} - \mathcal{K}_{TC\delta-1}^{-1} \mathcal{S}^{\top} - \mathcal{S} \mathcal{K}_{TC\delta-1}^{-1}]. \end{aligned} \quad (24)$$

It is well known that premultiplying a matrix  $A$  by a lower shift matrix results in the elements of  $A$  being shifted downward by one position, with zeroes appearing in the top row. Thus, in view of (24), we have that  $\mathcal{S} \mathcal{K}_{TC\delta-1}^{-1} \mathcal{S}^{\top}$  is a band matrix with bandwidth  $\delta - 1$ , while  $\mathcal{K}_{TC\delta-1}^{-1} \mathcal{S}^{\top} + \mathcal{S} \mathcal{K}_{TC\delta-1}^{-1}$  and thus  $\mathcal{K}_{TC\delta-1}^{-1}$  are band matrices with bandwidth  $\delta$ . ■

Also in this case one could try to find the closed form expression for  $\mathcal{K}_{TC\delta}$ , however its derivation is not straightforward from the case  $\delta = 2$ . On the other hand, we can define the corresponding finite dimensional kernel ma-

trix  $K_{TC\delta} \in \mathcal{S}_T$  as

$$[K_{TC\delta}]_{t,s} = [\mathcal{K}_{TC\delta}]_{t,s}, \quad t, s = 1 \dots T.$$

**Proposition 17** *The finite dimensional kernel  $K_{TC\delta}$  admits the following decomposition:*

$$K_{TC\delta}^{-1} = \kappa_{\delta}^{-1} F_T^{\delta} D_T (F_T^{\delta})^{\top}$$

where

$$D_T = \begin{bmatrix} D_{1,T} & 0 \\ 0 & B_T \end{bmatrix}$$

$$D_{1,T} = \text{diag}(\beta^{-1}, \beta^{-2}, \dots, \beta^{T-\delta}),$$

and  $B_T$  is a  $\delta \times \delta$  matrix. Thus,  $K_{TC\delta}^{-1}$  is banded of bandwidth  $\delta$ .

**Proof.** Let  $\mathcal{V}^{(j)} \in \mathbb{R}^{\infty \times T}$  denote a matrix whose first  $j - 1$  columns coincide with the null sequence and the remaining ones do not, thus  $\mathcal{V}^{(T+1)}$  is the null matrix. We use  $\sim$  to denote the equivalence relation  $\mathcal{X} \sim \mathcal{Y}$  which means that  $\mathcal{X} \in \mathbb{R}^{\infty \times T}$  and  $\mathcal{Y} \in \mathbb{R}^{\infty \times T}$  have the first columns (in the same number) equal to the null sequence and the other ones do not. Thus, the latter induces a splitting of  $\mathbb{R}^{\infty \times T}$  through the corresponding equivalence classes  $[\mathcal{V}^{(j)}] = \{\mathcal{X} \in \mathbb{R}^{\infty \times T} \text{ s.t. } \mathcal{X} \sim \mathcal{V}^{(j)}\}$  with  $1 \leq j \leq T + 1$ . In what follows, in order to ease the exposition (and thus with some abuse of notation) we use the symbol  $=$  instead of  $\sim$  in all the (submatrix) relations involving  $\mathcal{V}^{(j)}$ , with  $j = 1 \dots T + 1$ .

First, notice that  $\mathcal{F} = \mathcal{I} - \mathcal{S}$  and  $F_T = I_T - \mathcal{S}$  where  $\mathcal{S}$  and  $\mathcal{S}$  denote, respectively, the infinite and finite dimensional lower shift matrix. Recall that postmultiplying  $\mathcal{V}^{(j)}$ , with  $1 \leq j \leq T$ , by  $\mathcal{S}$  results in the columns of  $\mathcal{V}^{(j)}$  being shifted left by one position with a null sequence appearing in the last column position, thus

$$\mathcal{V}^{(j)} \mathcal{F} = \mathcal{V}^{(j-1)}; \quad (25)$$

premultiplying  $\mathcal{V}^{(j-1)}$ , with  $1 \leq j \leq T$ , by  $\mathcal{S}$  results in the rows of  $\mathcal{V}^{(j-1)}$  being shifted downward by one position with a null row vector appearing in the first top row, thus

$$\mathcal{S} \mathcal{V}^{(j-1)} = \mathcal{V}^{(j-1)}. \quad (26)$$

Combining (25)-(26), we obtain

$$\mathcal{V}^{(j)} \mathcal{F} = \mathcal{S} \mathcal{V}^{(j-1)}$$

and thus

$$\mathcal{F}^{-1} \mathcal{V}^{(j)} \mathcal{F} = \mathcal{V}^{(j-1)}, \quad 1 \leq j \leq T. \quad (27)$$

Then, we have

$$\mathcal{F}^{-1} \begin{bmatrix} I_T \\ \mathcal{V}^{(j)} \end{bmatrix} F_T = \begin{bmatrix} I_T \\ \mathcal{O} + \mathcal{F}^{-1} \mathcal{V}^{(j)} F_T \end{bmatrix} \quad (28)$$

where  $\mathcal{O} \in \mathbb{R}^{\infty \times T}$  is a matrix whose last column is a sequence of ones, while the other columns are null sequences, i.e.  $\mathcal{O} = \mathcal{V}^{(T-1)}$ . Accordingly, by (27)-(28) we have

$$\mathcal{F}^{-1} \begin{bmatrix} I_T \\ \mathcal{V}^{(j)} \end{bmatrix} F_T = \begin{bmatrix} I_T \\ \mathcal{V}^{(j-1)} \end{bmatrix}, \quad 1 \leq j \leq T+1. \quad (29)$$

Notice that

$$\begin{aligned} K_{TC\delta} &= \begin{bmatrix} I_T & 0 \end{bmatrix} \mathcal{K}_{TC\delta} \begin{bmatrix} I_T \\ 0 \end{bmatrix} \\ &= \kappa_\delta \begin{bmatrix} I_T & 0 \end{bmatrix} (\mathcal{F}^{-\delta})^\top \mathcal{D}^{-1} \mathcal{F}^{-\delta} \begin{bmatrix} I_T \\ 0 \end{bmatrix}. \end{aligned}$$

Consider

$$\begin{aligned} Y &:= (F_T^\delta)^\top K_{TC\delta} F_T^\delta \\ &= \kappa_\delta \mathcal{W}_\delta^\top \mathcal{D}^{-1} \mathcal{W}_\delta \end{aligned}$$

where

$$\mathcal{W}_\delta = \mathcal{F}^{-\delta} \begin{bmatrix} F_T^\delta \\ 0 \end{bmatrix} = \mathcal{F}^{-\delta} \begin{bmatrix} F_T^\delta \\ \mathcal{V}^{(T+1)} \end{bmatrix}.$$

Then, it remains to prove that  $Y = \kappa_\delta D_T^{-1}$ . Indeed,

$$\begin{aligned} \mathcal{W}_\delta &= \mathcal{F}^{-(\delta-1)} \mathcal{F}^{-1} \begin{bmatrix} I_T \\ \mathcal{V}^{(T+1)} \end{bmatrix} F_T F_T^{\delta-1} \\ &= \mathcal{F}^{-(\delta-1)} \begin{bmatrix} I_T \\ \mathcal{V}^{(T)} \end{bmatrix} F_T^{\delta-1} \\ &= \dots = \begin{bmatrix} I_T \\ \mathcal{V}^{(T+1-\delta)} \end{bmatrix} \end{aligned}$$

where we exploited (29). Thus,

$$\begin{aligned} Y &= \kappa_\delta \begin{bmatrix} I_T & (\mathcal{V}^{(T+1-\delta)})^\top \end{bmatrix} \mathcal{D}^{-1} \begin{bmatrix} I_T \\ \mathcal{V}^{(T+1-\delta)} \end{bmatrix} \\ &= \kappa_\delta \begin{bmatrix} I_T & (\mathcal{V}^{(T+1-\delta)})^\top \end{bmatrix} \begin{bmatrix} D_{1,T}^{-1} & 0 \\ 0 & \tilde{\mathcal{D}}^{-1} \end{bmatrix} \begin{bmatrix} I_T \\ \mathcal{V}^{(T+1-\delta)} \end{bmatrix} \\ &= \kappa_\delta (D_{1,T}^{-1} + (\mathcal{V}^{(T+1-\delta)})^\top \tilde{\mathcal{D}}^{-1} \mathcal{V}^{(T+1-\delta)}) = \kappa_\delta D_T^{-1} \end{aligned}$$

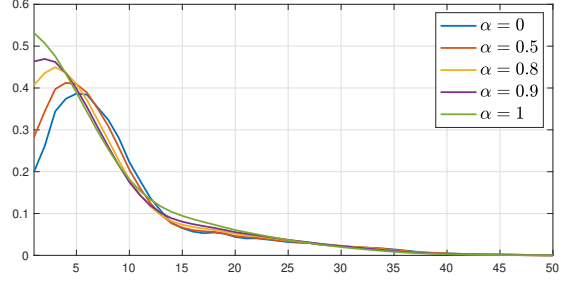


Fig. 4. One realization of  $g \sim \mathcal{N}(0, \lambda \mathcal{K}_{DC3})$  for different values of  $\alpha$ . Here,  $\beta = 0.8$  and  $\lambda = \|\mathcal{K}_{DC3}\|^{-1}$ .

where  $\tilde{\mathcal{D}} = \text{diag}(\beta^{T-\delta-1}, \beta^{T-\delta-2}, \dots)$ . ■

Finally, numerical experiments suggest that  $K_{TC\delta}$  is the maximum entropy extension of Problem 7 with  $c_{t,s} = [K_{TC\delta}]_{t,s}$  for  $|t-s| \leq \delta$ , i.e.  $K_{TC\delta}$  satisfies the conditions of Proposition 9.

It remains to design the DC kernel of order  $\delta$  connecting  $\mathcal{K}_{TC\delta-1}$  and  $\mathcal{K}_{TC\delta}$ . Drawing inspiration from Section 4 we define it as

$$\mathcal{K}_{DC\delta} = \kappa_\delta (\mathcal{F}_{\delta,\alpha} \mathcal{D} \mathcal{F}_{\delta,\alpha}^\top)^{-1} \quad (30)$$

where

$$\mathcal{F}_{\delta,\alpha} := (1 - \alpha) \mathcal{F}^{\delta-1} + \alpha \mathcal{F}^\delta$$

and  $\kappa_\delta$  is the normalization constant. Here,  $\eta = [\beta \ \alpha]^\top$  with  $0 < \beta < 1$  and  $0 \leq \alpha \leq 1$ . In Figure 2 we show a realization of the impulse response using (30) with  $\delta = 3$  as a function of  $\alpha$ ; as expected, the degree of smoothness increases as  $\alpha$  increases.

**Proposition 18** *The inverse of  $\mathcal{K}_{DC\delta}$  is a banded matrix of bandwidth  $\delta$ , that is  $[\mathcal{K}_{DC\delta}^{-1}]_{t,s} = 0$  for any  $|t-s| > \delta$ .*

**Proof.** First, for  $\delta = 1$   $K_{DC\delta}$  is the standard DC kernel whose inverse is tridiagonal, i.e. the statement holds. Finally, notice that

$$\mathcal{F}_{\delta,\alpha} := \mathcal{F}((1 - \alpha) \mathcal{F}^{\delta-2} + \alpha \mathcal{F}^{\delta-1}) = \mathcal{F} \mathcal{F}_{\delta-1,\alpha},$$

thus

$$\mathcal{K}_{DC\delta}^{-1} = \kappa_{\delta-1} \kappa_\delta^{-1} \mathcal{F} \mathcal{K}_{DC\delta-1}^{-1} \mathcal{F}^\top.$$

Accordingly, the remaining part of the proof is similar to the one of Proposition 16. ■

Also in this case the finite dimensional kernel  $K_{DC\delta} \in \mathcal{S}_T$  is defined as

$$[K_{DC\delta}]_{t,s} = [\mathcal{K}_{DC\delta}]_{t,s}, \quad t, s = 1 \dots T.$$

**Proposition 19** *The finite dimensional kernel  $K_{DC\delta}$  admits the following decomposition:*

$$K_{DC\delta}^{-1} = \kappa_\delta F_{\delta,\alpha,T} D_T (F_{\delta,\alpha,T})^\top$$

where

$$\begin{aligned} F_{\delta,\alpha,T} &= (1 - \alpha) F_T^{\delta-1} + \alpha F_T^\delta \\ D_T &= \begin{bmatrix} D_{1,T} & 0 \\ 0 & B_T \end{bmatrix} \\ D_{1,T} &= \text{diag}(\beta^{-1}, \beta^{-2}, \dots, \beta^{T-\delta}) \end{aligned}$$

and  $B_T$  is a  $\delta \times \delta$  matrix; Thus,  $K_{DC\delta}^{-1}$  is banded of bandwidth  $\delta$ .

**Proof.** The proof is similar to the one of Proposition 17.  $\blacksquare$

Also in this case numerical experiments suggest that  $K_{DC\delta}$  is the maximum entropy extension of Problem 7 with  $c_{t,s} = [K_{DC\delta}]_{t,s}$  for  $|t-s| \leq \delta$ .

Finally, this extension can be applied also to the high-frequency (HF) kernel, see Pilonetto & De Nicolao (2011):

$$[\mathcal{K}_{HF}]_{t,s} = (-1)^{|t-s|} \beta^{\max(t,s)} = (-1)^{|t-s|} [\mathcal{K}_{TC}]_{t,s}$$

where  $0 < \beta < 1$ . We define the high frequency kernel of order  $\delta \in \mathbb{N}$  as

$$[\mathcal{K}_{HF\delta}]_{t,s} = (-1)^{|t-s|} [\mathcal{K}_{TC\delta}]_{t,s}.$$

Moreover, we can define the high frequency diagonal-correlated (HC) kernel connecting  $\text{HF}\delta - 1$  and  $\text{HF}\delta$  as

$$[\mathcal{K}_{HC}]_{t,s} = (-1)^{|t-s|} [\mathcal{K}_{DC\delta}]_{t,s}.$$

It is straightforward to see that  $\mathcal{K}_{HF\delta}^{-1}$  and  $\mathcal{K}_{HC\delta}^{-1}$  are banded of bandwidth  $\delta$ , as well as their finite dimensional matrices  $K_{HF\delta}^{-1}$  and  $K_{HC\delta}^{-1}$ . It is possible to find the closed form expression for the Cholesky factor and the determinant of  $K_{HF2}^{-1}$  and  $K_{HC2}^{-1}$ . Finally,  $K_{HF2}$  and  $K_{HC2}$  are, respectively, the maximum entropy solution of a band extension problem similar to the ones introduced in Section 5.

## 7 Frequency analysis

An exponentially convex local stationary (ECLS) kernel  $\mathcal{K} \in \mathcal{S}_\infty$  admits the following decomposition

$$[\mathcal{K}]_{t,s} = \beta^{\frac{t+s}{2}} [\mathcal{W}]_{t,s} \quad (31)$$

where  $\mathcal{W} \in \mathcal{S}_\infty$  is a stationary kernel, i.e. the covariance function of a stationary process and thus  $[\mathcal{W}]_{t,s} = [\mathcal{W}]_{t+k,s+k}$  for any  $k \in \mathbb{N}$ . Recall that TC, DC and SS are ECLS kernels. It is straightforward to see that TC2 and DC2 are ECLS kernel whose stationary parts are, respectively,

$$\begin{aligned} [\mathcal{W}_{TC2}]_{t,s} &= 2\beta^{\frac{|t-s|}{2}+1} + (1-\beta)(1+|t-s|)\beta^{\frac{|t-s|}{2}} \\ [\mathcal{W}_{DC2}]_{t,s} &= \frac{\beta^{\frac{|t-s|}{2}}(1-(1-\beta)\alpha^{|t-s|+1}) - \alpha^2\beta^{\frac{|t-s|}{2}+1}}{1-\alpha}. \end{aligned}$$

**Theorem 20** *TC $\delta$  and DC $\delta$  kernels with  $\delta > 2$  are ECLS, that is*

$$\mathcal{K}_{TC\delta} = \beta^{\frac{t+s}{2}} [\mathcal{W}_{TC\delta}]_{t,s}, \quad \mathcal{K}_{DC\delta} = \beta^{\frac{t+s}{2}} [\mathcal{W}_{DC\delta}]_{t,s}$$

where  $\mathcal{W}_{TC\delta}$  and  $\mathcal{W}_{DC\delta}$  are stationary kernels.

**Proof.** We only prove the claim for TC $\delta$  because the one for DC $\delta$  is similar. By (23), we have that

$$\mathcal{K}_{TC\delta} = \kappa_\delta \mathcal{X}^\top \mathcal{D}^{-1} \mathcal{X} \quad (32)$$

where  $\mathcal{X} = \mathcal{F}^{-\delta} = (\mathcal{F}^{-1})^\delta$ . Since  $\mathcal{F}$  is lower triangular, Toeplitz and invertible, then by Lemma 2 we know that  $\mathcal{F}^{-1}$  is lower triangular and Toeplitz. Accordingly,  $\mathcal{X}$  is lower triangular and Toeplitz because it is given by a product of lower triangular and Toeplitz matrices. Hence, let

$$\mathcal{X} = \text{Tpl}(x_1, x_2, x_3, \dots).$$

Moreover,

$$[\mathcal{X}]_{t,:} = [0 \dots 0 \underbrace{x_1 \ x_2 \ x_3 \dots}_{t\text{-th element}}].$$

Taking into account (32), we have

$$\begin{aligned} [\mathcal{K}_{TC\delta}]_{t,s} &= \kappa_\delta [\mathcal{X}]_{t,:} \mathcal{D}^{-1} [\mathcal{X}]_{s,:}^\top \\ &= \kappa_\delta \sum_{k=1}^{\infty} \beta^{\max(t,s)+k-1} x_k x_{k+|t-s|} \\ &= \beta^{\frac{t+s}{2}} \underbrace{\kappa_\delta \sum_{k=1}^{\infty} \beta^{\frac{|t-s|}{2}+k-1} x_k x_{k+|t-s|}}_{:= [\mathcal{W}_{TC\delta}]_{t,s}} \quad (33) \end{aligned}$$

where we have exploited the fact that  $\max(t,s) = (t+s)/2 + |t-s|/2$ . It is straightforward to see that  $\mathcal{W}_{TC\delta}$  is a stationary kernel. In view of (31) and (33), we conclude that TC $\delta$  is ECLS.  $\blacksquare$

Although it is not immediate to derive the closed form expression for  $\mathcal{W}_{TC\delta}$  and  $\mathcal{W}_{DC\delta}$ , we can compute them

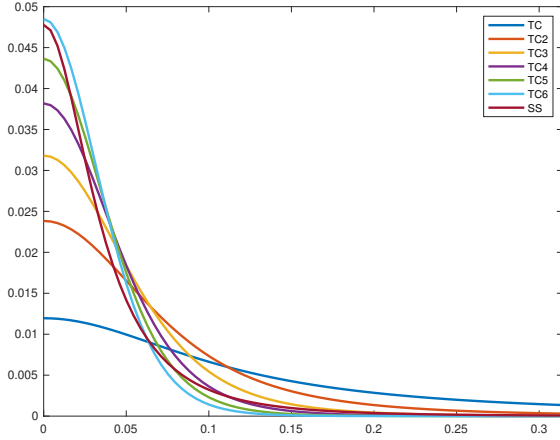


Fig. 5. Power spectral density of the stationary part of TC,  $TC\delta$ , with  $\delta = 2 \dots 6$ , and SS with  $\beta = 0.8$ . All those power spectral densities are normalized to one in order to ease the comparison.

numerically:

$$[W_{TC\delta}]_{t,s} \approx \beta^{-\frac{t+s}{2}} [K_{TC\delta}]_{t,s}$$

and likewise for  $DC\delta$ . Clearly, the larger  $T$  is, the better the approximation above is.

Therefore, it is interesting to compare the frequency content in their stationary parts. In doing that, we recall that

$$[W]_{t,s} = \frac{1}{2\pi} \int_{-\pi}^{\pi} \phi(\vartheta) \cos(\vartheta(t-s)) d\vartheta$$

where  $\phi(\vartheta)$ , with  $\vartheta \in [0, 2\pi]$ , is the power spectral density of the (stationary) process. In order to compare SS with the others we need to choose  $\gamma = \sqrt[3]{\beta}$  in (8); in this way the latter has the exponential part as in (31). Figure 5 shows the power spectral densities of the stationary part of TC,  $TC\delta$ , with  $\delta = 2 \dots 6$  and SS. As expected, the higher  $TC\delta$  is, the more statistical power is concentrated for frequencies close to zero. TC2 promote less smoothness than SS, while the latter is more similar to TC5 and TC6. It is worth noting that we can plot also the power spectral density corresponding to  $DC\delta$ . The latter smoothly changes from the one of  $TC\delta - 1$ , with  $\alpha = 0$ , to the one of  $TC\delta$ , with  $\alpha = 1$ .

Finally, also  $HF\delta$  and  $HC\delta$  are ECLS kernels. Figure 6 shows the power spectral density of the stationary part of HF and  $HF\delta$  for  $\delta = 2 \dots 4$ . The higher  $\delta$  is, the more the statistical power is concentrated for frequencies close to  $\pi$ .

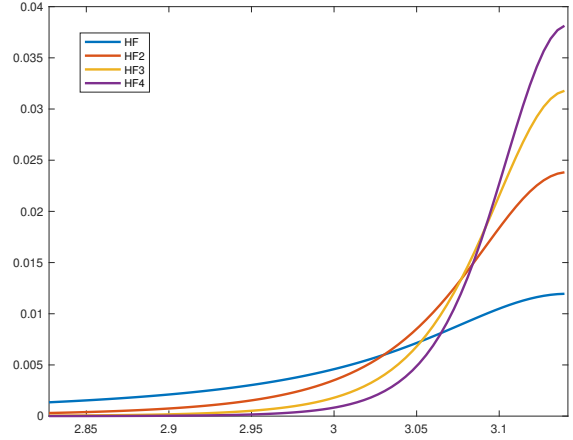


Fig. 6. Power spectral density of the stationary part of HF and  $HF\delta$ , with  $\delta = 2 \dots 4$ , with  $\beta = 0.8$ . All those power spectral densities are normalized to one in order to ease the comparison.

## 8 Numerical experiments

We compare the proposed kernels in two Monte Carlo studies. The first Monte Carlo study is composed by 200 experiments. In each experiment we generate the impulse response  $g$  with practical length  $T = 50$  as follows:

$$g_t = \sum_{k=1}^3 a_k \cos(b_k t + c_k)$$

where its parameters are drawn as follows:  $a_k \in \mathcal{U}([0.8, 0.9])$ ,  $b_k \in \mathcal{U}([0.4, 0.5])$  and  $c_k \in \mathcal{U}([0, \pi])$ . Figure 7 (top) shows ten realizations drawn from such process. Then, we generate the input of length  $N = 500$  using the MATLAB function `idinput.m` as a realization from a Gaussian noise with band  $[0, 0.2]$ . Then, we feed the corresponding system (1) with it obtaining the dataset  $D^N := \{y(t), u(t)\}_{t=1}^N$ . Here,  $\sigma^2$  is chosen in such a way that the signal to noise ratio is equal to one. Then, we estimate the impulse response using the following estimators:

- $\hat{g}_{DI}$  is the estimator in (2) using the diagonal kernel (4);
- $\hat{g}_{DC}$  is the estimator in (2) using the DC kernel (6) where the hyperparameter  $\alpha$  is constrained to belong to the interval  $[0, 1]$  in order to make a fair comparison with the  $DC\delta$  kernel;
- $\hat{g}_{TC}$  is the estimator in (2) using the TC kernel (5);
- $\hat{g}_{SS}$  is the estimator in (2) using the SS kernel (8);
- $\hat{g}_{DC\delta}$  is the estimator in (2) using the  $DC\delta$  kernel (30) with  $\delta = 2 \dots 6$ ;
- $\hat{g}_{TC\delta}$  is the estimator in (2) using the  $TC\delta$  kernel (23) with  $\delta = 2 \dots 6$ .

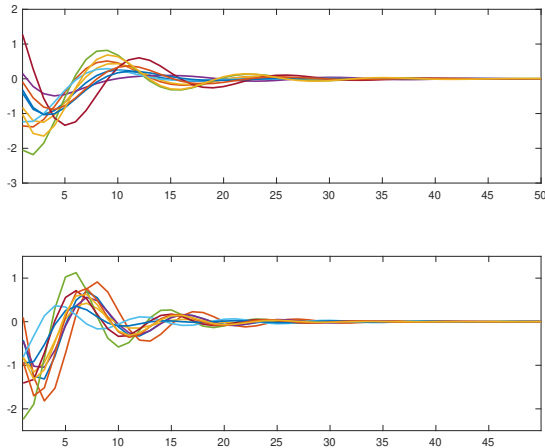


Fig. 7. *Top panel.* Ten realizations of the impulse response in the first Monte Carlo study. *Bottom panel.* Ten realizations of the impulse response in the second Monte Carlo study.

For all these estimators the kernel hyperparameters are obtained by minimizing the negative log-marginal likelihood (3). Finally, for each estimator we compute the average impulse response fit

$$\text{AIRF} = 100 \left( 1 - \frac{\|g - \hat{g}\|}{\|g - \bar{g}\|} \right)$$

where  $\bar{g} = \sum_{t=1}^T g_t$  and  $\hat{g}$  is the corresponding estimator. Clearly, the more AIRF is close to 100, the better the estimator performance is. Figure 8 shows the boxplot of AIRF for the estimators. The best ones are  $\hat{g}_{DC\delta}$  and  $\hat{g}_{TC\delta}$  with  $\delta = 3$ ;  $\hat{g}_{TC\delta}$ , with  $\delta = 2, 4, 5, 6$ ,  $\hat{g}_{DC\delta}$ , with  $\delta = 4, 5, 6$ , and SS perform slightly worse; the remaining estimators exhibit the worst performance. This result is not surprising, indeed, the impulse responses in this Monte Carlo study are very smooth, see Figure 7 (top).

The second Monte Carlo study is likewise to the previous one but  $a_k \sim \mathcal{U}([0.63, 0.73])$ . In plain words, the generated impulse responses are less smooth than before, see Figure 7 (bottom). The boxplot of the average impulse response fit for the estimators is depicted in Figure 9. The best performance is achieved by  $\hat{g}_{DC2}$ ;  $\hat{g}_{TC2}$  and  $\hat{g}_{SS}$  are slightly worse. The worst one is  $\hat{g}_{TC6}$ , while  $\hat{g}_{DI}$  is the worst one among the kernels inducing less smoothness than  $\hat{g}_{DC2}$ . Indeed, the former induces too much smoothness on the impulse response, while the latter too less smoothness.

We conclude that the best kernel structure depends on how smooth is the true impulse response. Moreover, SS and TC2 provide a similar performance, thus the latter can be safely replaced by TC2 whose hyperparameters can be computed efficiently as explained in Section 5.3.

## 9 Conclusions

We have introduced a second-order extension to TC and DC kernels called TC2 and DC2, respectively. The latter induce more smoothness than the former. Moreover, TC2 and DC2 have their inverse which is a pentadiagonal matrix. We have derived their closed form expression for the determinant and the Cholesky factorization of the inverse matrix. These kernels also have a meaningful interpretation: they are the maximum entropy solution, respectively, of a band extension problem. This idea can be extended for higher-orders: for instance, we have proved that the inverse of the kernel is still banded. Finally, numerical experiments showed that TC2 and SS perform in a similar way. Accordingly, TC2 represents an appealing alternative to SS because it admits an efficient implementation for searching the optimal hyperparameters through marginal likelihood.

## References

- Akaike, H. (1974). A new look at the statistical model identification. *IEEE Transactions on Automatic Control*, 19, 716–723.
- Ardeshiri, T., & Chen, T. (2015). Maximum entropy property of discrete-time stable spline kernel. In *IEEE International Conference on Acoustics, Speech and Signal Processing (ICASSP)* (pp. 3676–3680).
- Carli, F. P. (2014). On the maximum entropy property of the first-order stable spline kernel and its implications. In *IEEE Conference on Control Applications (CCA)* (pp. 409–414).
- Carli, F. P., Chen, T., & Ljung, L. (2017). Maximum entropy kernels for system identification. *IEEE Transactions on Automatic Control*, 62, 1471–1477.
- Carli, F. P., Chiuso, A., & Pillonetto, G. (2012). Efficient algorithms for large scale linear system identification using stable spline estimators. *IFAC Proceedings Volumes*, 45, 119–124.
- Chen, T. (2018). Continuous-time dc kernel—a stable generalized first-order spline kernel. *IEEE Transactions on Automatic Control*, 63, 4442–4447.
- Chen, T., & Andersen, M. S. (2021). On semiseparable kernels and efficient implementation for regularized system identification and function estimation. *Automatica*, 132, 109682.
- Chen, T., Andersen, M. S., Mu, B., Yin, F., Ljung, L., & Qin, S. J. (2018). Regularized LTI system identification with multiple regularization matrix. *Ifac-papersonline*, 51, 180–185.
- Chen, T., Ardeshiri, T., Carli, F. P., Chiuso, A., Ljung, L., & Pillonetto, G. (2016). Maximum entropy properties of discrete-time first-order stable spline kernel. *Automatica*, 66, 34–38.
- Chen, T., & Ljung, L. (2013a). Implementation of algorithms for tuning parameters in regularized least squares problems in system identification. *Automatica*, 49, 2213–2220.

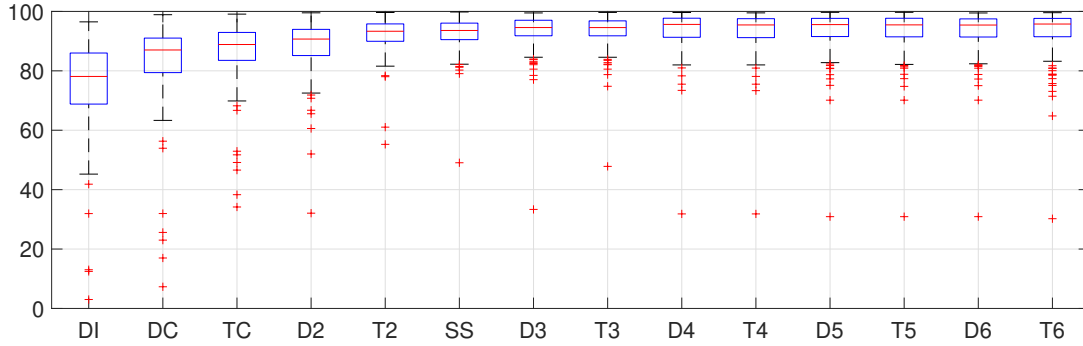


Fig. 8. Average impulse response fit in the first Monte Carlo study composed by 200 experiments.

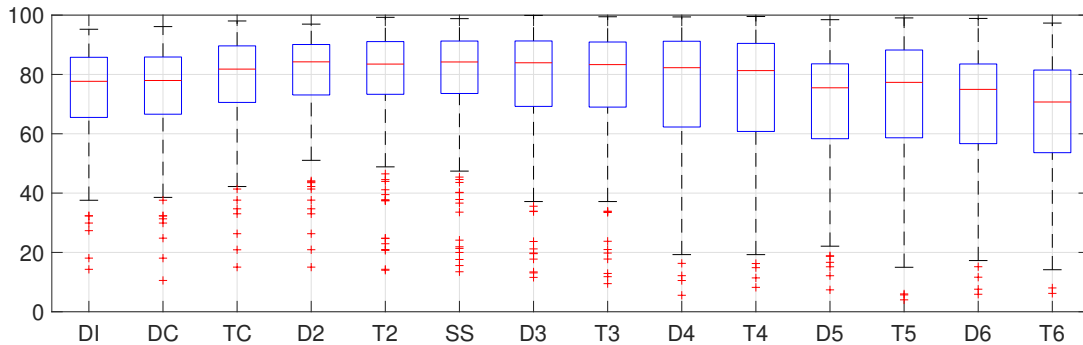


Fig. 9. Average impulse response fit in the second Monte Carlo study composed by 200 experiments.

- Chen, T., & Ljung, L. (2013b). Implementation of algorithms for tuning parameters in regularized least squares problems in system identification. *Automatica*, 49, 2213–2220.
- Chen, T., & Ljung, L. (2015a). On kernel structures for regularized system identification (i): a machine learning perspective. *IFAC-PapersOnLine*, 48, 1035–1040.
- Chen, T., & Ljung, L. (2015b). On kernel structures for regularized system identification (ii): A system theory perspective. *IFAC-PapersOnLine*, 48, 1041–1046.
- Chen, T., Ohlsson, H., & Ljung, L. (2012). On the estimation of transfer functions, regularizations and gaussian processes-revisited. *Automatica*, 48, 1525–1535.
- Chiuso, A., & Pillonetto, G. (2012). A Bayesian approach to sparse dynamic network identification. *Automatica*, 48, 1553–1565.
- Dempster, A. P. (1972). Covariance selection. *Biometrics*, 28, 157–175.
- Dinuzzo, F. (2015). Kernels for linear time invariant system identification. *SIAM Journal on Control and Optimization*, 53, 3299–3317.
- Dym, H., & Gohberg, I. (1981). Extensions of band matrices with band inverses. *Linear algebra and its applications*, 36, 1–24.
- Ford, N. J., Savostyanov, D. V., & Zamarashkin, N. L. (2014). On the decay of the elements of inverse Triangular toeplitz matrices. *SIAM Journal on Matrix Analysis and Applications*, 35, 1288–1302.
- Fujimoto, Y. (2021). Efficient implementation of kernel regularization based on ADMM. In *SYSID*.
- Gohberg, I., Goldberg, S., & Kaashoek, M. A. (1993). *Classes of linear operators* volume 63. Birkhäuser.
- Jorgesen, P., Kornelson, K., & Shuman, K. (2011). *Iterated Function Systems, Moments, and Transformations of Infinite Matrices*. American Mathematical Society.
- Ljung, L. (1999). *System Identification: Theory for the User*. New Jersey: Prentice Hall.
- Marconato, A., Schoukens, M., & Schoukens, J. (2017). Filter-based regularisation for impulse response modelling. *IET Control Theory & Applications*, 11, 194–204.
- Pillonetto, G., & De Nicolao, G. (2010). A new kernel-based approach for linear system identification. *Automatica*, 46, 81–93.
- Pillonetto, G., & De Nicolao, G. (2011). Kernel selection in linear system identification part i: A gaussian process perspective. In *50th IEEE Conference on Decision and Control and European Control Conference* (pp. 4318–4325).
- Pillonetto, G., Dinuzzo, F., Chen, T., De Nicolao, G., & Ljung, L. (2014). Kernel methods in system identification, machine learning and function estimation: A survey. *Automatica*, 50, 657–682.
- Rasmussen, C., & Williams, C. (2006). *Gaussian Processes for Machine Learning*. The MIT Press.

- Schwarz, G. (1978). Estimating the Dimension of a Model. *The Annals of Statistics*, 6, 461–464.
- Söderström, T., & Stoica, P. (1989). *System Identification*. Hemel Hempstead, UK: Prentice-Hall International.
- Wahba, G. (1990). *Spline models for observational data*. SIAM.
- Zorzi, M. (2020). A new kernel-based approach for spectral estimation. In *European Control Conference (ECC)* (pp. 534–539).
- Zorzi, M., & Chiuso, A. (2015). A Bayesian approach to sparse plus low rank network identification. In *Proceedings of the IEEE Conference on Decision and Control* (pp. 7386–7391). Osaka.
- Zorzi, M., & Chiuso, A. (2017). Sparse plus low rank network identification: A nonparametric approach. *Automatica*, 76, 355–366.
- Zorzi, M., & Chiuso, A. (2018). The harmonic analysis of kernel functions. *Automatica*, 94, 125–137.